HHS Public Access

Author manuscript

Crit Care Med. Author manuscript; available in PMC 2017 August 01.

Published in final edited form as:

Crit Care Med. 2016 August ; 44(8): e633–e638. doi:10.1097/CCM.0000000000001625.

High Intracranial Pressure Induced Injury in the Healthy Rat Brain

Xingping Dai, MD, PhD[1,2], **Olga Bragina, MS**[1], **Tongsheng Zhang, PhD**[3], **Yirong Yang, PhD**[4], **Gutti R. Rao, MD**[5], **Denis Bragin, PhD**[1], **Gloria Statom, MSBME**[1], and **Edwin M. Nemoto, PhD**[1]

[1]Department of Neurosurgery, University of New Mexico, Albuquerque, NM 87131

[2]Department of Integrated Traditional Chinese and Western Medicine, Xiangya Hospital, Central South University, Changsha, Hunan, China 410078

[3]Department of Neurology, University of New Mexico, Albuquerque, NM 87131

[4]College of Pharmacy, University of New Mexico, Albuquerque, NM 87131

[5]Department of Pathology & Laboratory Medicine, VA Pittsburgh Health Care System Pittsburgh, PA 15240

Abstract

Objective—We recently showed that increased intracranial pressure (ICP) to 50 mmHg in the healthy rat brain results in microvascular shunt (MVS) flow characterized by tissue hypoxia, edema and increased blood brain barrier permeability. We now determined whether increased ICP results in neuronal injury by Fluoro-Jade stain (FJS) and whether changes in cerebral blood flow (CBF) and cerebral metabolic rate for oxygen ($CMRO_2$) suggest nonnutritive MVS flow.

Design—Intracranial pressure was elevated by a reservoir of artificial cerebrospinal fluid (CSF) connected to the cisterna magna. Arterial blood gases, cerebral arterial-venous oxygen content difference (CAVDO2) and cerebral blood flow (CBF) by magnetic resonance imaging (MRI) were measured. FJS neurons were counted in histological sections of the right and left dorsal and lateral corticies and hippocampus.

Setting—University laboratory

Edwin M. Nemoto, PhD (Corresponding Author and address for reprints): Department of Neurosurgery, University of New Mexico, 1101 Yale Blvd, NE, Domenici Hall/ BRaIN Center, Rm 1131B Tel: 505-272-5990, ENemoto@salud.unm.edu.
Xingping Dai, MD, PhD, Institute of Integrated Traditional Chinese and West Medicine, Xiangya Hospital, Central South University, Changsha, Hunan 410078, P.R.China, Phone: (0086) 731-84539698, xingpingdai@salud.unm.edu
Olga Bragina, MS, Department of Neurosurgery, University of New Mexico, MSC10 5615, 1 University of New Mexico, Albuquerque, NM 87131, Phone: 505-272-0156, Obragina@salud.unm.edu
Tongsheng Zhang, PhD, Department of Neurology, University of New Mexico, Brain Imaging Center, UNM Domenici Hall, MSC10 5620, 1101 Yale Boulevard NE, Albuquerque, NM 87106, Office Phone: (505) 272-6053, TZhang@salud.unm.edu
Yirong Yang, PhD, College of Pharmacy, University of New Mexico, Albuquerque, NM, Brain Imaging Center, UNM Domenici Hall, MSC10 5620, 1101 Yale Boulevard NE, Albuquerque, NM 87106, Office Phone: (505) 272-6053, YiYang@salud.unm.edu
Gutti S. Rao, MD, Department of Pathology & Laboratory Medicine, VA Pittsburgh Health Care System, University Drive C, Pittsburgh, PA 15240, Phone: 412-360-6549, Gutti.Rao@va.gov
Denis E. Bragin, PhD, Department of Neurosurgery, University of New Mexico, MSC10 5615, 1 University of New Mexico, Albuquerque, NM 87131, Phone: 505-925-7628, dbragin@salud.unm.edu
Gloria Statom, MSBME, Department of Neurosurgery, University of New Mexico, MSC10 5615, 1 University of New Mexico, Albuquerque, NM 87131, Phone: 505-272-0107, Gstatom@salud.unm.edu

Subjects—Male Sprague Dawley rats.

Interventions—Arterial pressure support if needed by i.v. dopamine infusion and base deficit corrected by sodium bicarbonate.

Measurements and Main Results—FJS neurons increased 2.5 and 5.5 fold at ICP of 30 and 50 mmHg; CPP of 57 ± 4 (mean ± SEM) and 47 ± 6 mmHg, respectively, ($P<0.001$); highest in the right and left cortices. Voxel frequency histograms of CBF showed a pattern consistent with MVS flow by dispersion to higher CBF at high ICP and decreased $CMRO_2$.

Conclusions—High ICP likely caused neuronal injury due to a transition from normal capillary flow to nonnutritive MVS flow resulting in tissue hypoxia, edema and manifest by a reduction in $CMRO_2$.

Keywords

Cerebral blood flow; Cerebral Arteriovenous oxygen difference; Fluoro-Jade stain; Intracranial hypertension; Ischemia; Microvascular Shunting

Introduction

The clinical intracranial pressure (ICP) threshold triggering implementation of ICP lowering maneuvers such as osmotherapy, hyperventilation, 30° head up tilt, cerebrospinal fluid (CSF) drainage, and ICP lowering drugs, is 20 to 25 mmHg as recommended by the Brain Trauma Guidelines and the Lund Concept, at a CPP target range of 50-70 mmHg (1,2). These thresholds were adopted from observations in patients suffering traumatic brain injury (TBI) or cerebrovascular accidents (CVA) that showed poor prognosis and outcome at ICP >20-25 mmHg (3). However, brain injury after TBI and CVA represents a complex interaction of pathophysiologic and metabolic processes do not directly address the question of the tolerance of the *healthy or normal brain* uncomplicated by injury, to elevated ICP.

Our studies showed that the critical CPP identified at high ICP fell from 50 to 30 mmHg when CPP was lowered by increasing ICP instead of lowering mean arterial pressure (MAP) (4,5). We subsequently showed that the critical CPP of the cerebral circulation obtained by increasing ICP was accurately identified as 50 mmHg by dopamine-induced ICP reactivity (iPRx) and cerebrovascular reactivity (iCVRx) (6). The apparent lower critical CPP at high ICP was attributable to a transition from normal capillary to microvascular shunt (MVS) flow as previously hypothesized (14).

We showed for the first time, a progressive transition from normal capillary flow to MVS flow with increasing ICP in the healthy rat brain (7,8). This transition to nonnutritive shunt flow raised the question as to whether high ICP without brain injury will induce neuronal injury. Our aim in this study was to determine whether high ICP causes neuronal injury in the healthy rat brain as evaluated by Fluoro-Jade B staining capable of detecting early neuronal degeneration independent of the cause of injury (9). Cerebral blood flow (CBF) measured by magnetic resonance imaging (MRI) arterial spin labeling (ASL) was used to determine whether evidence of MVS flow could be observed based on voxel-wise distribution of CBF frequency histograms.

Methods

This study was conducted according to protocol # 100907 approved by the University of New Mexico Institutional Animal Care and Use Committee. Male Sprague Dawley rats (300-450 g body weight, Harlan Laboratories, Indianapolis, IN) were laboratory acclimated for seven days.

A. Anesthesia and Surgical Procedures

Anesthetsia was induced in a plastic box insufflated with 4% isoflurane/68% nitrous oxide and 28% oxygen. They were intubated with a 14G × 1.9″ catheter and their lungs mechanically ventilated (Harvard Apparatus, Holliston, MA) on 2% isoflurane/29% oxygen/69% nitrous oxide; tidal volume, 2.5mL at a rate of 60/min. Rectal temperature was continuously monitored and kept at 37.5 ± 0.5 °C by a heated water blanket. Atropine (0.54 mg, i.p.) was administered to reduce mucous secretions. Femoral artery and vein catheters (PE-50) were used to monitor arterial blood pressure on a laptop computer with data acquisition software (BIOPAC, Goleta, CA) and blood sampling (0.2 ml each) and for fluid replacement (Lactated Ringers, one ml/hr, i.v.).

In a right lateral position, a PE 30 catheter was inserted into the left internal maxillary vein with the tip of the catheter at the outflow of the left transverse sinus for cerebral venous blood (0.2 ml per sample) sampling as previously described (10,11). Bovine heparin (50 IU) was injected retrograde immediately after insertion into the catheter and transverse sinus to prevent clotting.

In a sterotaxic head frame (Kopf Instruments, Inc.), a catheter (PE-30) was inserted and glued (cyanoacrylate glue) into the cisterna magna. ICP was continuously monitored and manipulated by adjusting the height of a reservoir of artificial cerebrospinal fluid (ACSF) above the head of the rat. In a leak-free system, ICP could be precisely controlled and maintained at a constant level. In MRI studies the rats were removed from the stereotaxic frame and placed into the cradle of a 4.7T Bruker MRI scanner as described below.

B. Experimental Protocol

Rats were studied in three groups with ICP maintained at 10 (control) 30 and 50 mmHg (Table 1). Arterial and cerebral venous oxygen content ($CAVDO_2$) measurements were obtained at baseline and at the start and end of each hour. The blood samples were analyzed with a GEM4000 (Instrumentation Laboratories, Bedford, MA) for direct spectrophotometric measurement of hemoglobin oxygen content and electrolytes, blood gases, pH and base excess. In the control, normal ICP group, ICP remained unchanged for two hours with arterial and transverse sinus blood gas measurements after each hour. In the 30 and 50 mmHg ICP groups, ICP was elevated to 30 or 50 mmHg after 30 min at control of 10 mmHg. In some rats where the Cushing reflex was not sufficiently robust to maintain CPP at the desired level, Dopamine (Hospira Inc, Lake Forest, IL) was infused i.v. at doses ranging from 20 to 120 μg/min as reported in a previous study (8). Arterial and venous blood gases and $CAVDO_2$ measurements were made after each hour. At the end of the two-hour period of normal or elevated ICP, the rats brains were transcardially perfused with 40 ml

phosphate buffered solution (PBS) followed by 40 ml of 4% paraformaldehyde. Brains were removed from the calvaria, postfixed for 24 hr in 4% PFA followed by cryoprotection in 30% sucrose and frozen for histopathology.

a) Magnetic Resonance Imaging—The MRI scanner was a 4.7-Tesla (Bruker Biospin; Billerica, MA, USA), equipped with a 40-cm bore, a 660mT/m (rise time within 120μs) gradient and shim systems. RF signal transmission and reception was done with a small-bore linear RF coil (Inner Diameter = 72mm) and a single tuned surface coil (RAPID Biomedical, Rimpar, Germany).

T2-weighted images were acquired with a fast spin-echo sequence (RARE) (TR/TE = 5000ms/56ms, FOV=4cm×4cm, slice thickness=1mm, interslice distance = 1.1mm, number of slice = 12, matrix = 256×256, number of average = 3). Multi-slice, multi-shot, diffusion-weighted echo-planar imaging (EPI) (TR/TE=3800ms/38ms; b-values=600 and 1900 s/mm2 in 30 directions; FOV = 4cm×4cm, slice thickness=1mm, matrix = 256 × 256) was performed to assess tissue architecture. Cerebral blood flow (CBF) was measured using arterial spin labeling (ASL). The sequence: Flow-sensitive Alternating Inversion Recovery Rapid Acquisition with Relaxation Enhancement (FAIR-RARE) was used to implement ASL with parameters: TE/TR=46ms/16000ms, FOV=4cm×4cm, slice thickness=1mm, number of slice=1, matrix=128×128.

In the MRI scanner, arterial blood pressure and rectal temperature were continuously monitored and arterial and cerebral venous blood gases were intermittently obtained at the start and end of each ICP episode.

b) MRI Cerebral Blood Flow (CBF) Analysis—An in-house-developed program in Matlab (Mathworks, MA) by TZ was used to analyze the MRI CBF data. In our experimental protocol, the various MRI sequences were scanned sequentially. For efficient posthoc analysis, the MRI database generated by the scanner was searched based on the protocol used in the scan to find the corresponding data sets. Then an exponential fitting was carried out pixel-by-pixel for parameter T1 or T2 by means of the values found in the data. The resultant image data was then saved and processed for voxel analysis as previously described (12).

a) Fluoro-Jade B staining

The sections (35 μm) were washed in 0.1 M neutral phosphate buffer, mounted on slides and air dried on a slide warmer at 50° C. The sections were immersed in 1% sodium hydroxide in 80% alcohol, followed by 70% alcohol and in distilled water. The sections were transferred to a solution of 0.06% potassium permanganate, rinsed in distilled water and placed in staining solution (0.0004% solution of Fluoro-Jade B in 0.1 % acetic acid). The sections were washed in distilled water for one minute three times and air dried on a slide warmer at 50 degrees C. The dried sections were cleared by immersion in xylene and cover slipped with DPX.

Images were taken in six areas of interest on the left and right dorsal and lateral cortices and left and right CA1 regions of the hippocampus, using 10× objective of an Olympus TH

4-100 inverted microscope (supplementary Fig. 1). These images at 10X were used for *blinded quantitation* of the number of dead neurons in one coronal section of the rat brain at the level of the hippocampus . The total sum and average number of stained dead neurons were counted on each of the 10X sections.

2. Statistical Analysis

Statistical data analysis was done using GraphPad Prism version 6.0software (GraphPad Software, Inc., La Jolla, CA 92037). Descriptive statistics and parametric analyses were done by ordinary one-way ANOVA and t-tests. Analysis of non-parametric data in the comparison of frequency histograms was done by Mann-Whitney U test for analysis of differences in frequency histograms. Significant differences were tested by the student's t test with a minimum P value of 0.05.

Results

Among all animals combined in the three ICP groups, ICP was significantly ($P<0.001$) increased from means of 11 ± 3 to 29 ± 3 and 50 ± 0 mmHg while CPP decreased from 84 ± 7 to 57 ± 16 and 49 ± 19 mmHg, respectively (Table 1). All other physiological variables were similar between the ICP groups. Arterial glucose levels were equally elevated in all groups likely due to surgical stress. Normal arterial blood glucose in the rat is 125 mg% (13). Base excess was within normal limits and unchanged between groups despite an apparent increase from -1.9 ± 2.3 to -5.0 ± 5.5 mEq/l.

Illustrations of Fluoro-Jade B staining showed dead neurons at ICP of 50 mmHg and CPP of 70 mmHg in the dorsal cortex in Fig. 1 (A) and CA1 region of the hippocampus (B) but not in the neocortex (C) or the CA1 region of the hippocampus (D) at normal ICP of 10 mmHg and CPP of 80 mmHg.

Increased ICP to 30 and 50 mmHg increased the sum and average number of dead neurons in the 18 regions of the cortex and hippocampus (supplementary Fig 2). The number of dead neurons in the dorsal and lateral hippocampus increased by three-fold from an ICP of 10 mmHg to 30 mmHg and by nine fold at 50 mmHg. The average number of dead neurons was not significantly higher at ICP of 30 mmHg but significant ($P< 0.01$) at 50 mmHg compared to ICP of 10 mmHg.

The number of FJ stained neurons in each of the six brain regions illustrated in the coronal section (supplementary Fig. 1) at mean ICP of 11 (Fig. 2A), 29 (Fig. 2B) and 50 mmHg (Fig. 2C) and CPP of 84, 57 and 49 mmHg increased significantly ($P=0.0001$) comparing all regions at each ICP. All regions of the brain examined showed increased neuronal injury. The cortices showed the greatest number of injured neurons.

CBF for both averaged whole brain and voxel analyses were obtained from cortical and striatal regions of interest (supplementary Fig. 3). The frequency distribution of bilateral cortical, hippocampus and striatal voxel-wise CBF shows values of coronal sections in bins of 10 ml/100g/min from zero to 405 ml/100g/min (X-axis values are X 10) divided into 5 different ICP and CPP groups (Fig. 3). Control ICP at 10 mmHg (blue) at a CPP of 86

mmHg. At an ICP of 30 mmHg, CPP was 47 (red) or 73 (green) mmHg. At an ICP of 50 mmHg, CCP was 66 (purple) and 30 (orange) mmHg. Increasing ICP from 10 to 30 mmHg at a CPP of 47 mmHg compressed the CBF distribution to the left from a peak of 100 to 60 ml/100g/min. Increasing CPP to 73 mmHg dispersed CBF to higher values with a peak at 180 ml/100g/min and CBF ranging from 200 to 300 mls/100g/min. Increasing ICP to 50 mmHg at a CPP of 66 mmHg decreased the distribution of CBF to lower values compared to the control ICP of 10 mmHg and CPP of 86 mmHg. Decreasing CPP to 30 mmHg at an ICP of 50 mmHg increased the distribution to higher CBF values suggesting greater MVS flow at high ICP and lower CPP.

Whole brain $CMRO_2$ decreased ($P<0.005$) at ICP of 30 and 50 mmHg compared to control of 10 mmHg (Fig. 4) whereas global CBF (supplementary Fig. 4) was significantly ($P=0.01$) decreased at an ICP of 50 but not 30 mmHg compared to control.

Discussion

Our studies show that in the healthy uninjured brain, increasing ICP to 30 and 50 mmHg with CPP maintained within acceptable clinical range of 60 and 50 mmHg, induces neuronal injury as characterized by neuronal degeneration by Fluoro-Jade B staining. Changes in CBF frequency histograms at increased ICP and at lower and higher CPP suggests that the neuronal injury may be attributable to the development of nonnutritive MVS flow resulting in tissue hypoxia and edema as previously shown by two photon laser scanning microscopy (7).

MVS flow is also suggested by voxel analyzed CBF frequency histograms showing a distribution to higher CBF at ICP of 30 and 50 mmHg that was CPP dependent. $CMRO_2$ was significantly reduced at ICP of both 30 and 50 mmHg by almost 50% while global CBF was significantly reduced at an ICP of 50 mmHg but not 30 mmHg. The reduction in $CMRO_2$ and the broadening of the voxel CBF frequency histograms at high ICP suggest nonnutritive MVS flow at high ICP.

The normal values for $CMRO_2$ we report with mean values of 4.5 ml/100g/min are lower than the 5.5 ml/100g/min values we previously reported (10,11). However in the earlier study, $CMRO_2$ measurements were made in rats on 70% nitrous oxide/ 30% oxygen anesthesia whereas in this study, we used 2.0% isoflurane/69% nitrous oxide/29% oxygen anesthesia explaining the 20% decrease in $CMRO_2$.

As previously hypothesized (14), the mechanism of the injury induced by high ICP is likely due to increased cerebral venous pressure resulting in pericapillary edema, increased capillary resistance to where capillary rarefaction occurs and flow is diverted to MVS ranging in diam > 8 to 45 μm as opposed to capillaries > 3 to 8 μm diameter (15,16). In earlier studies on pigs, we showed that as ICP is increased, cerebral venous pressure increases in parallel and remains higher than ICP as long as perfusion through the tissue continues (14) verifying earlier studies (17,18). The fact that cerebral venous pressure *must* exceed ICP in the perfused brain is an important concept that is not generally appreciated.

Thus, as pericapillary edema develops capillary resistance increases to the point where the increase in capillary resistance exceeds that for MVS. We suggest that MVS exists in the normal brain (15, 16) but are unperfused because of the lower resistance of the larger cross sectional area of the capillary bed. We also surmise that the increase in capillary resistance due to pericapillary edema could occur in a contusion whereby brain edema and increased capillary resistance leads to a rapid transition to MVS flow.

Increasing ICP elicited the Cushing reflex with an increase in arterial pressure and did not require dopamine infusion to maintain CPP. However, in a few studies, Dopamine infusion was used to maintain CPP. The use of dopamine as the vasopressor of choice had been previously determined because norepinephrine and phenylephrine both induced severe acidosis (7). Dopamine infusion did not influence the transition from capillary to microvascular shunt flow. We showed that increasing CPP by i.v. Dopamine infusion decreased rather than increased MVS flow (8).

Lafrenayae and associates (19) reported that persistent increase in ICP alone without compromised CPP results in what they referred to as “microporation” and neuronal plasmalemmal perturbation that could “precipitate persistent neuronal impairment and ultimately neuronal death” and a direct effect of high ICP on neuronal plasma membrane injury. Thus, while our results ascribes the detrimental effects of increased ICP in the healthy brain to a transition to nonnutritive MVS flow, Lafrenayae and associates suggest that the increase in ICP directly impacts the neuronal plasmalemmal permeability which leads to neuronal degeneration. The observation of capillary rarefaction in ischemic brain injury in patients (20-22) and the rarefaction of capillaries in the infarcted brain (23) coincides with observations of capillary fallout as an important process in the pathogenesis of neuronal injury at increased ICP.

Our findings on the effect of high ICP on normal brain tissue are relevant to idiopathic intracranial hypertension (IIH) and pseudo tumor cerebri syndrome (PTCS) where maximum CSF opening pressures of up to 50 mmHg have been reported (24-26). Although there is no patient data on ischemic neuronal change early after onset of IIH, there is clear evidence of neurologic dysfunction and infarction, which may be seen as lacunar infarcts, may actually represent cavitation of infarcted tissue in normal pressure hydrocephalus where venous obstruction may be responsible (27, 28). The ischemic injury suffered in IIH is attributed to increased venous pressure which is precisely what we suggested occurs with high ICP (14). It has been observed that IIH patients tend to be younger child bearing aged obese women supporting the notion of increased venous outflow resistance.

In summary, we have shown that increased ICP to 30 and 50 mmHg at CPP of 60 and 50 mmHg, respectively, causes significant neuronal injury likely due to a transition from capillary to MVS flow. The effect of high ICP on the injured brain requires further examination for its possible direct relationship to the loss of CBF autoregulation which may represent a transition to MVS flow resulting in an open transmission of the elevated ICP to the cerebral venous system, the brain parenchyma and the exacerbation of brain edema.

Supplementary Material

Refer to Web version on PubMed Central for supplementary material.

Acknowledgments

None

Financial Support; The China Scholarship Council Grant # 201206375041 to Dr. Xingping Dai; AHA 12BGIA11730011; NIH Grants NS061216, NS051639 and UNM HSC COBRE program (P20 RR15636); NIH-NINDS CoBRE Pilot Project P30GM103400; UNM SOM Dedicated Health Research Fund Pilot Project; and the Department of Neurosurgery.

References

1. Bratton SL, Chestnut RM, Ghajar J, et al. Guidelines for the management of severe traumatic brain injury. VIII. Intracranial pressure thresholds. J Neurotrauma. 2007; 24(Suppl 1):S55–8. [PubMed: 17511546]
2. Grande PO, Asgeirsson B, Nordstrom CH. Volume-targeted therapy of increased intracranial pressure: the Lund concept unifies surgical and non-surgical treatments. Acta Anaesthesiol Scand. 2002; 46:929–41. [PubMed: 12190792]
3. Balestreri M, Czosnyka M, Hutchinson P, et al. Impact of intracranial pressure and cerebral perfusion pressure on severe disability and mortality after head injury. Neurocrit Care. 2006; 4:8–13. [PubMed: 16498188]
4. Miller JD, Stanek A, Langfitt TW. Concepts of cerebral perfusion pressure and vascular compression during intracranial hypertension. Prog Brain Res. 1972; 35:411–32. [PubMed: 5009562]
5. Grubb RL Jr, Raichle ME, Phelps ME, et al. Effects of increased intracranial pressure on cerebral blood volume, blood flow, and oxygen utilization in monkeys. J Neurosurg. 1975; 43(4):385–98. [PubMed: 808593]
6. Bragin DE, Statom GL, Yonas H, et al. Critical cerebral perfusion pressure at high intracranial pressure measured by induced cerebrovascular and intracranial pressure reactivity. Crit Care Med. 2014; 42(12):2582–90. [PubMed: 25289933]
7. Bragin DE, Bush RC, Muller WS, et al. High intracranial pressure effects on cerebral cortical microvascular flow in rats. J Neurotrauma. 2011; 28:775–85. [PubMed: 21395499]
8. Bragin DE, Bush RC, Nemoto EM. Effect of cerebral perfusion pressure on cerebral cortical microvascular shunting at high intracranial pressure in rats. Stroke. 2013; 44(1):177–81. [PubMed: 23204051]
9. Schmued LC, Albertson C, Slikker W Jr. Fluoro-Jade: a novel fluorochrome for the sensitive and reliable histochemical localization of neuronal degeneration. Brain Res. 1997; 751:37–46. [PubMed: 9098566]
10. Nemoto EM, Klementavicius R, Yonas H. Effects of hypothermia on cerebral metabolic rate for oxygen. J Neurosurg Anesthesiol. 1994; 6(3):220–3. [PubMed: 8081102]
11. Nemoto EM, Klementavicius R, Melick JA, Yonas H. Suppression of cerebral metabolic rate for oxygen (CMRO2) by mild hypothermia compared with thiopental. J Neurosurg Anesthesiol. 1996; 8(1):52–9. [PubMed: 8719194]
12. Foley LM, Hitchens TK, Barbe B, et al. Quantitative temporal profiles of penumbra and infarction during permanent middle cerebral artery occlusion in rats. Transl Stroke Res. 2010; 1(3):220–9. [PubMed: 21666857]
13. Ishiwata Y, Sanada Y, Yasuhara M. Effects of gatifloxacin on serum glucose concentration in normal and diabetic rats. Biol Pharm Bull. 29:527–31. [PubMed: 16508159]
14. Nemoto EM. Dynamics of cerebral venous and intracranial pressures. Acta Neurochir Suppl. 2006; 96:435–7. [PubMed: 16671500]

15. Hasegawa T, Ravens JR, Toole JF. Precapillary arteriovenous anastomoses. “Thoroughfare channels” in the brain. Arch Neurol. 1967; 16(2):217–24. [PubMed: 4163498]
16. Ravens, JR. Anastomoses in the vascular bed of the human cerebrum. In: Cervos-Navaro, J., editor. Pathology of Cerebral Microcirculation. Walter de Gruyter; Berlin: 1974. p. 16-38.
17. Nakagawa Y, Tsuru M, Yada K. Site and mechanism for compression of the venous system during experimental intracranial hypertension. J Neurosurg. 974(41):427–434.
18. Yada K, Nakagawa Y, Tsuru M. Circulatory disturbance of the venous system during experimental intracranial hypertension. J Neurosurg. 1973; (39):723–729. [PubMed: 4759659]
19. Lafrenaye AD, McGinn MJ, Povlishock JT. Increased intracranial pressure after diffuse traumatic brain injury exacerbates neuronal somatic membrane poration but not axonal injury: evidence for primary intracranial pressure-induced neuronal perturbation. J Cereb Blood Flow Metab. 2012; 32:1919–32. [PubMed: 22781336]
20. Kuwabara H, Ohta S, Brust P, et al. Density of perfused capillaries in living human brain during functional activation. Prog Brain Res. 1992; 91:209–15. [PubMed: 1410406]
21. Gjedde A, Kuwabara H, Hakim AM. Reduction of functional capillary density in human brain after stroke. J Cereb Blood Flow Metab. 1990; 10(3):317–26. [PubMed: 2329120]
22. Chantler PD, Shrader CD, Tabone LE, et al. Cerebral cortical microvascular rarefaction in metabolic syndrome is dependent on insulin resistance and loss of nitric oxide bioavailability. Microcirculation. 2015 May 25. [Epub ahead of print]. doi: 10.1111/micc.12209
23. Tomita, M. Significance of cerebral blood volume. In: Tomita, M.; Sawada, T.; Naritomi, H.; Heiss, WD., editors. Cerebral hyperemia and Ischemia: From the standpoint of Cerebral Blood Volume. Elsevier Science Publishers BV (Biomedical Division); 1988. p. 3-31.
24. Andrews LE, Liu GT, Ko MW. Idiopathic intracranial hypertension and obesity. Hormone Res Paediatr. 2014; 81:217–25.
25. Higgins JN, Cousins C, Owler BK, et al. Idiopathic intracranial hypertension: 12 cases treated by venous sinus stenting. J Neurol Neurosurg Psychiatry. 2003; 74:1662–6. [PubMed: 14638886]
26. Dwyer CM, Prelog K, Owler BK. The role of venous sinus outflow obstruction in pediatric idiopathic intracranial hypertension. J Neurosurg Pediatr. 2013; 11:144–9. [PubMed: 23176141]
27. Bateman GA. The pathophysiology of idiopathic normal pressure hydrocephalus: cerebral ischemia or altered venous hemodynamics? Am J Neuroradiol. 2008:198–203. [PubMed: 17925373]
28. Lenfeldt N, Larsson A, Nyberg L, Birgander R, Eklund A, Malm J. Diffusion tensor imaging reveals supplementary lesions to frontal white matter in idiopathic normal pressure hydrocephalus. Neurosurgery. 2011:1586–93. [PubMed: 21336219]

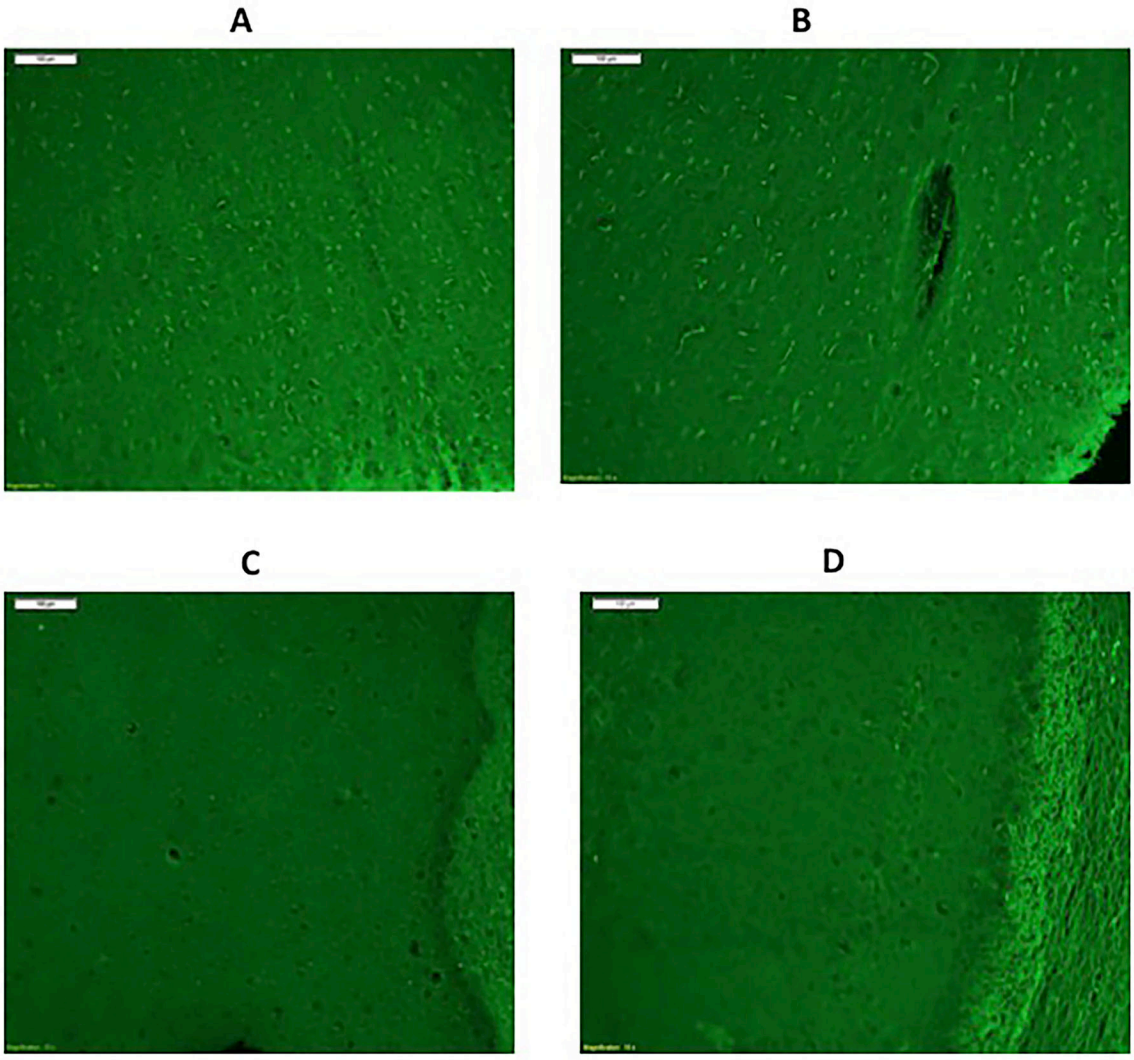

Figure 1.

Micrograph image (10X) of Fluoro-Jade B stained images of (A) the left dorsal cortex after two hours at ICP of 50 mmHg and CPP of 70 mmHg; and (B) the CA1 region of the hippocampus at ICP 50, CPP 70 for two hours. (C) right dorsal cortex of a rat maintained at an ICP 10 mmHg, CPP 80 mmHg for two hours and (D) the right hippocampus at an ICP of 10 and CPP of 80 mmHg.

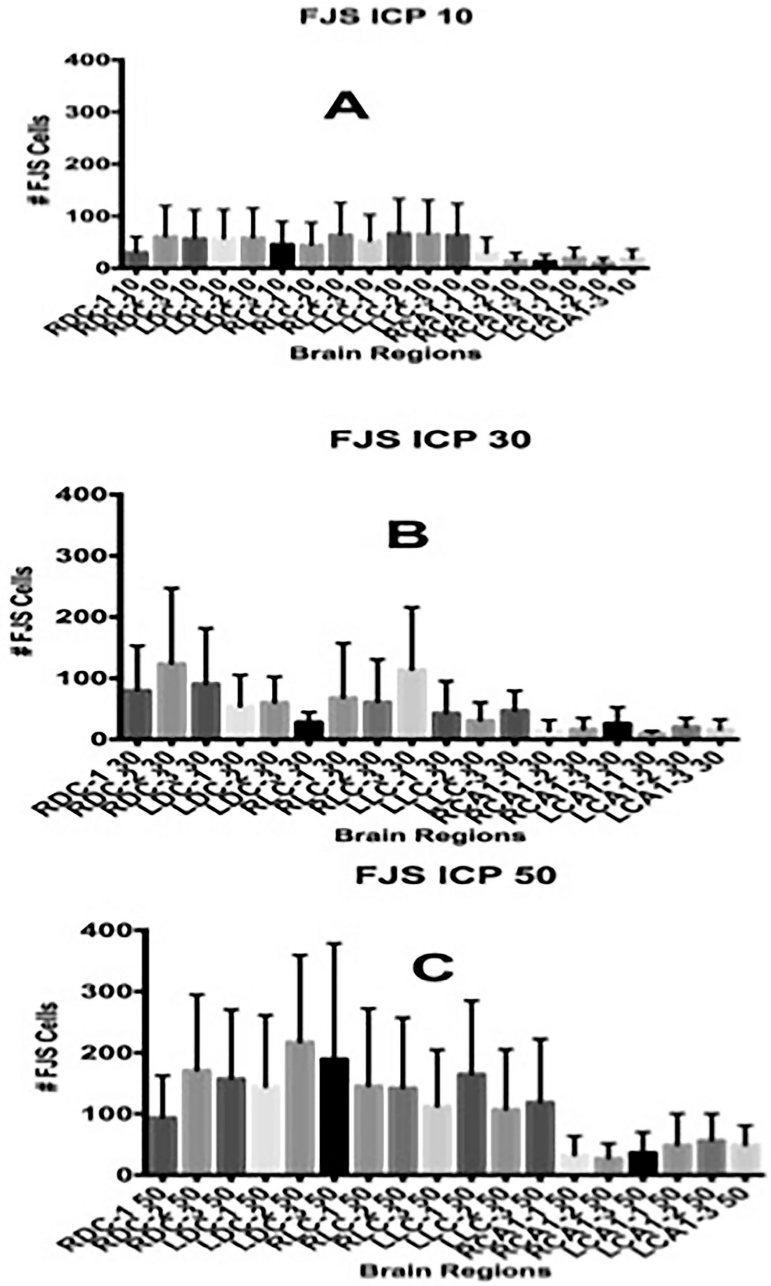

Figure 2.

Number of Fluoro-Jade stained (FJS) neurons in the three sections taken from the right and left, dorsal and lateral cortices and hippocampus (see Fig. 1) at ICP of 10 (A), 30 (B) and 50 (C) mmHg. The differences in the number of neurons between ICP 10 and 30 and 50 mmHg were highly significant (P=0.001) by one-way ANOVA.

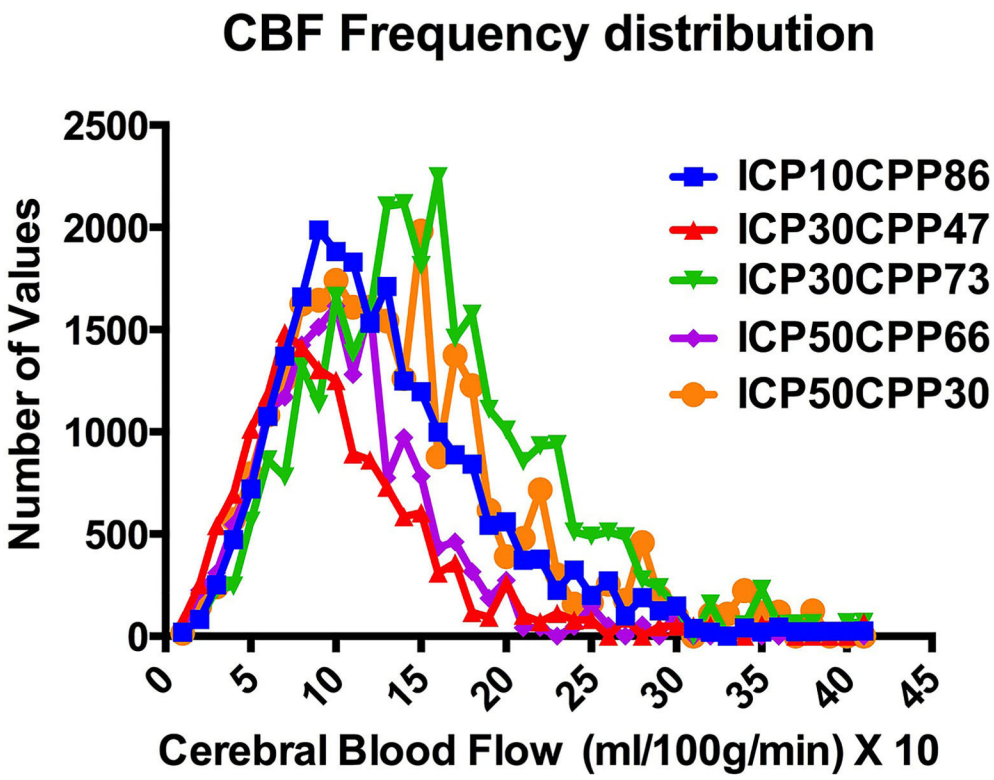

Figure 3.

Interaction between intracranial pressure (ICP) and cerebral perfusion pressure (CPP) on the frequency distribution of cerebral blood flow (CBF). The frequency distribution at normal ICP of 10 mmHg and CPP of 86 mmHg in blue shows that increasing ICP to 30 mmHg at CPP of 47 mmHg shifts the CBF distribution from about 100 ml/1000g/min to a peak at 60 ml/100g/min. Increasing CPP to 73 mmHg at an ICP of 30 mmHg CBF distribution to a peak of about 180 ml/100g/min with a wider distribution to 200 and 300 ml/00g/min. Increasing ICP to 50 mmHg at a CPP of 66 mmHg restores the distribution but at a lower peak flow and decreasing CPP to 30 mmHg to a wider distribution and higher peak flow values. The increased distribution of CBF to high values and increase in the peak of the CBF frequency distribution suggests increased microvascular shunting.

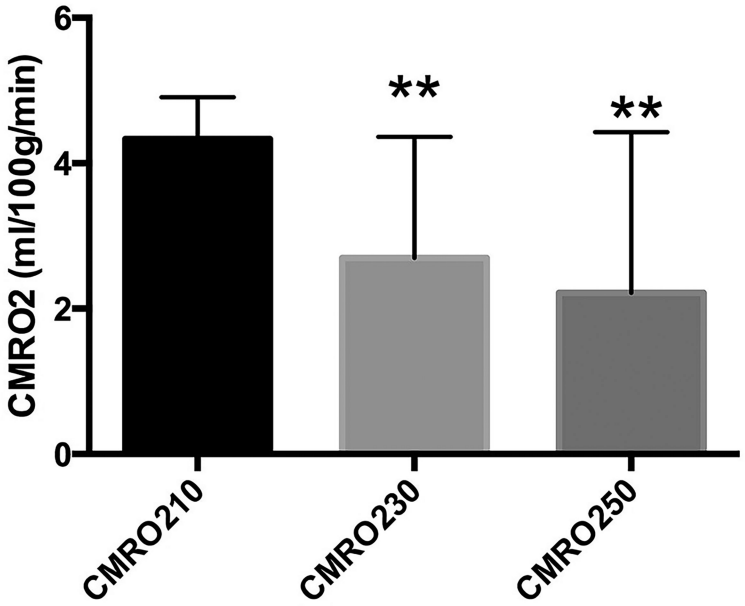

Figure 4.

Whole brain cerebral metabolic rate for oxygen ($CMRO_2$), ml/100g/min in rats at ICP of 10 (N=12), 30 (N=6), and 50 (N=5) mmHg. **P<0.006 compared to ICP of 10 mmHg.

Table 1

Averaged physiological variables in rats subjected to intracranial pressures of 10, 30 and 50 mmHg.

	ICP	CPP	MAP	pH	PCO_2	PO_2	GLU	LAC	BE
	(mmHg)	(mmHg)	(mmHg)		(mmHg)	(mmHg)	mg%	μM/L	mEq/L
m±sd	11 ±3	84±7	95±5	7.38±0.09	40±8	127±41	258±48	1.5±2.2	-1.9±2.3
n	16	16	16	16	16	16	16	16	16
m±sd	29±3**	57±16**	86±16	7.37±0.1	37±8	127±22	225±55	2.6±2.5	-3.4±2.8
n	11	11	11	19	19	19	19	16	19
m±sd	50±0**	49±19**	97±19	7.30±0.1	37±8	121±23	290±77	2.2±3.1	-5.0±5.5
n	15	15	16	15	15	15	15	15	15

** P=0.001